



## Effect of Intensity Measure on the Response of a 3D-Structure under Different Ground Motion Duration

H. Rajabnejad, H. Hamidi\*, S. A. Naseri, M. A. Abbaszadeh

Faculty of Civil Engineering, Babol Noshirvani University of Technology, Babol, Iran

### PAPER INFO

#### Paper history:

Received 16 May 2021  
Received in revised form 03 July 2021  
Accepted 04 July 2021

#### Keywords:

Intensity Measure  
Ground Motion Duration  
Seismic Parameters  
Residual Inter-story Drift  
Correlation Coefficient

### ABSTRACT

In seismic performance assessment of structures, the features of ground motion (GM) duration on the response of building structures remain vague and have inconclusive results. Also, intensity measures (IMs) link the ground motion hazard with the structural response; hence, using a suitable IM plays a significant role in the prediction of structural response. In this research, the effect of strong ground motion duration and the correlation coefficient of different intensity measures on the residual inter-story drift (RIDR) of a three-dimensional steel structure were investigated. Using nonlinear dynamic analyses and a total number of 34 earthquake records, the relationship between short- and long-duration seismic parameters including amplitude, energy, and frequency content parameters were investigated. The correlation between the 14 selected scalar intensity measures and the RIDR of the structure was also investigated. The results showed the highest correlation between the seismic parameters, such as Peak ground acceleration (PGA), Housner Intensity (HI), and Velocity spectrum intensity (VSI), with other seismic parameters in both short- and long-duration strong ground motions. Based on the maximum residual inter-story drift index, Mehanny and Cordova index ( $IM_C$ ), Bojórquez and Iervolino index ( $I_{NP}$ ), and the geometric mean of  $S_a$  ( $S_{a_{ave}}$ ) intensity measures represented the least dispersion versus long-duration records. On the other hand,  $I_{NP}$ , Spectra acceleration at the period of  $T_1$  ( $S_a(T_1)$ ), and  $S_{a_{ave}}$  intensity measures showed the least dispersion versus short-duration records.

doi: 10.5829/ije.2021.34.10a.04

## 1. INTRODUCTION

Two recent earthquakes in Chile, Maule (2010,  $M_w = 8.8$ ), and Tohoku, Japan (2011,  $M_w = 9$ ) have caused major structural failures. The earthquake records had some unique features (long duration) compared to other similar records happening in different parts of the world. The effect of earthquake duration on structures has attracted significant attention in recent decades. Considering how much and how long duration can directly affect the seismic response of structures, this study might be of high importance [1].

In general, since severe earthquakes tend to be recorded at many stations, each with different site conditions, every earthquake may be recorded with different characteristics. One of the most important properties, which is different in each station, is the strong

ground motion duration. Due to the possibility of occurring earthquakes with similar severity in the coming years, a precise and comprehensive study on such earthquakes and their effects on different areas seems to be valuable [2–5].

Raghunandan et al. [2] evaluated the risk of the collapse of structures in a subduction region. Chandramohan et al. [6] found that the probability of collapse of the structure would rise by the increases in the strong ground motion duration. Barbosa et al. [7] studied the effect of duration of strong ground motion on the damage of steel structures using two damage indices. The results indicated more extensive damage to the structure under long-duration earthquakes. As a result, energy dissipation would become unavoidable. So as to reduce resistance and stiffness, using nonlinear quantitative finite element components; Chandramohan et al. [6] and Barbosa et al. [7] obtained a coefficient. The coefficient

\*Corresponding Author Institutional Email: [h.hamidi@nit.ac.ir](mailto:h.hamidi@nit.ac.ir) (H. Hamidi)

was applied to investigate the impact of strong ground motion duration. In other research studies, where the cumulative increase of power is taken into account, it was seen that the rise in duration of strong ground motion led to a rise in the accumulation of damage to the structure [6,7]. Ruiz-Garcia [8] analyzed residual displacements caused by earthquakes with long strong ground motion duration and the results showed that ground motion duration did not have an important impact on the amplitude of peak residual drift demands in MDOF systems; but, records having a long duration tended to grow residual drift demands in the upper stories of long-period generic frames [8]. In studies conducted by Song et al. [9], Foschaar et al. [10], Raghunandan and Liel [11], Hancock and Bommer [12] and Zhang et al. [13], the probability of building collapse under both short- and long-duration ground motions were surveyed. The collapse probability of buildings was compared over the long and short duration of ground motion [9–13]. In a study by Bommer et al. [14], Iervolino et al. [15], and Bojorquez et al. [16] on the effect of strong ground motion on seismic response of structures, the direct effect of strong ground motion duration on maximum IDR was pointed out. Nassar and Krawinkler [17], Shome et al. [18], Tremblay, and Atkinson [19], and Chai [20] worked on the small effect of the duration of strong ground motion on the seismic response of structures. Bhargavi et al. [21] introduced a coefficient that can be utilized to rate the damage potential of any strong ground motion record regardless of the extent and region of the earthquake.

Bradley [22] evaluated the correlation between the mean time of strong ground motion and the range of cumulative intensities in order to select records. The results showed that ignoring the duration of strong ground motion in selecting accelerations may contribute to the scattered seismic response of the analysis. Zhou et al. [23] studied the effect of strong ground motion duration on reducing the damping factor and proposed a coefficient to modify the reduction damping coefficient. Nevertheless, in most of the studies on the duration of strong ground motion, both in the cases mentioned and in cases not mentioned here, modeling was either one or two-dimensional using the linear and nonlinear approaches. In a few studies, the structural responses were evaluated using three-dimensional models [24]. Some studies have pointed out the direction of using vector-valued intensity measures as a way to overcome this issue [6,25–27]. Yakhchalian et al. [28] with investigating the capability of different intensity measures (IMs), including  $S_a(T_1)$ , as a common scalar IM and twelve vector-valued IMs for seismic collapse assessment of structures showed that using the new vector-valued IM leads to a more trustworthy seismic collapse assessment of structures. Kassem et al. [29] studied the efficiency of an improved seismic vulnerability index and concluded that variation in

estimating the intensity measure might lead to uncertainties associated with a vulnerability assessment. Kassem et al. [30] in a study investigated on the quantification of collapse margin of a retrofitted university building in Beirut using three different strong ground motion duration. Farsangi et al. [31] considered the effect of coinciding horizontal and vertical ground excitations on the collapse margins of non-ductile structure using a general array of ground motions was chosen from the PEER NGA-WEST2 and Iran Strong Motions Network database. Nazri et al. [32] in investigating *Probabilistic of Structural Pounding Between Adjacent Buildings* obtained that structural damage is directly proportional to ground motion intensity.

In previous studies, the correlation of the response of structures with different intensities was examined, and in these studies, the frequency content, record duration, and other seismic parameters were different from each other. In this study, firstly, the records were examined which were very similar in terms of frequency content due to the similarity of the shape of the first mode spectrum, and secondly, the effect of strong ground motion duration on the *residual drift* values was investigated, which has not been studied in the past. Therefore, the simultaneous effect of the *uniformity of frequency contents*, and the study of *residual drift* values at different *intensities* were investigated in an experimentally verified real-scale structure for the first time in this study.

Accordingly, the effect of strong ground motion duration on the response of a real scale verified three-dimensional steel structure was investigated regarding

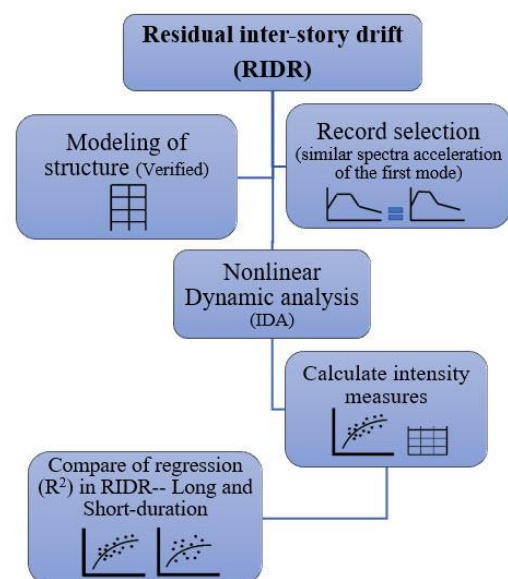


**Figure 1.** The process of determining and comparing the residual inter-story drift at long- and short- duration

different types of intensity measures. Two sets of long- and short-duration natural earthquake records were used to find out the effect of strong ground motion duration on seismic response of the abovementioned structure. Then, the effect of different intensity measures on the response of the structure was evaluated and the adequacy of the intensity measures was calculated. Using correlation coefficients, the dependency of seismic parameters was also studied. A summarized process for determination and comparison the residual inter-story drift at long- and short- duration is shown in Figure 1.

## 2. INTENSITY MEASURES

Parameters that quantify earthquake strengths are called "Intensity Measure". Selecting an appropriate intensity measure is important since the seismic performance of structures can be predicted more realistically in different engineering aspects such as nonlinear assessment and probabilistic seismic hazard analysis [33]. The importance of Intensity Measure (IM) results from associating seismic hazard analysis with seismic analysis of structures. Choosing an appropriate intensity measure can make a seismic evaluation of the structure more realistic. IM, a parameter that quantifies the strength of an earthquake, is a measure of the severity of probabilistic risk analysis used in seismic analysis of structures.

In other words, the IM is responsible for establishing a link between seismic hazard analysis and seismic analysis of structures. An appropriate IM tends to contain some characteristics, the most important of which are efficiency and severity of the measure [34]. Efficient Intensity measure is an intensity measure that is capable of predicting the response of structures at low dispersion. Many studies have been conducted on new intensity measures and comparison of the existing ones. One of the most commonly used intensity measures used to design and evaluate the seismic performance of structures is the pseudo-acceleration spectrum at first mode;  $S_a(T_1)$ . Due to its convenient usage, many researchers have used it to evaluate the structures seismically. Another common intensity measure is the peak ground acceleration (PGA), which highly correlates with spectral acceleration components at low-frequency times. Lee et al. [35] developed fragility curves in masonry and concrete structures with high frequency using PGA. In 1998, Shome et al. [18] showed that using  $S_a(T_1)$  instead of PGA would improve the reliability of results.

Peak Ground Velocity (PGV) and Peak Ground Displacement (PGD) are other commonly used intensity measures. Although  $S_a(T_1)$  is most widely used, it is less reliable when used in the nonlinear behavior range of a structure than in the linear behavior of structure. An increase in the period due to nonlinear behavior causes

the structure to be influenced by a different response spectrum from the one in the first mode ( $T_1$ ). That is why researchers have proposed intensity measures that can accommodate parts of the response spectrum that would affect the response of the nonlinear behavior of structure. In 2004, Cordova et al. [36] proposed an intensity measure that, in addition to the spectral acceleration component during the first mode of a structure, would consider a component of spectral acceleration when the period was more than the first period of the first mode of structure. Bojórquez and Iervolino [37] suggested the  $I_{NP}$  intensity measure to evaluate the seismic performance of structures. Soleymani [38] investigated effects between intensity measures and three structural damage indicators containing the Bracci index, the modified flexural damage ratio index and the drift index for different ground motion. In this intensity measure, a part of the response spectrum that can have a significant effect on the nonlinear behavior of the structure is considered to be the part of the intensity measure. In this study, as shown in Table 1, the intensity measures were investigated.

## 3. LONG- AND SHORT- DURATION GROUND MOTIONS SET

The definitions of strong ground motion based on acceleration are divided into three broad categories, which are briefly presented in the following, with the other parts of definitions being based on the response to earthquake forces.

The first group is called Bracket Duration. The total time elapsed between the first and last passage of a certain level of acceleration is known as the duration of the bracket [39]. One of the disadvantages of this definition is that it only considers the first and the last level while ignoring the characteristics of the strong shake section. As a result, it is possible to calculate long, strong ground motion duration in earthquakes with both pre and post-shocks [40]. The second group is called Uniform Duration. In this definition, instead of the time between the first and last passage of a specific acceleration level, the total sum of the times in which the acceleration value exceeds this threshold is considered. Although this definition is less sensitive to the desired level in terms of bracket duration, it does not provide a sustained duration of the strong ground motion. The last group that is based on acceleration is called "significant duration". It is based on the accumulation of energy in acceleration and is expressed as the square integral of acceleration, velocity, or displacement of the earth. If ground speed is used to calculate the integral, the calculated value can depend on energy density [41]; and if acceleration is used in the integration, the value obtained is the Arias intensity, which is the most common definition for strong motion duration [42]. The content of

the significant duration has the advantage of taking into account the characteristics of the entire acceleration and calculating the continuum time, which might be strong ground motion. The definitions are generally based on the duration of earthquakes, and the acceleration applied to the structures is not considered. Therefore, a method that considers the amounts of acceleration applied to the structures would improve the results.

Chandramohan et al. [6] used long and short duration records categories to classify records. The  $D_{5-75\%}$  index was used to describe the time of strong ground motion, which at first was shown by Foschaar et al. [10]. This

might be a good definition of distinct short and long-term ground motions. Chandramohan et al. [6] collected 2000 paired accelerations of some of the world's strong earthquakes in order to select long and short records. The accelerations were filtered using Boore and Bommer methods [43, 44]. In each acceleration, the spectral acceleration was plotted between 0.05 and 6 seconds. At intervals of every 0.05 seconds, a total of 120 points of spectral acceleration was selected to calculate points  $L_1, L_2, L_3 \dots$  and  $L_{120}$ , with the mean value of  $\bar{L}$  for the long duration acceleration and points  $S_1, S_2, S_3 \dots$  and  $S_{120}$

**TABLE 1.** The definition of the applied Intensity Measures (IMs)

Category	Name	Definition
Frequency response based IMs	$Sa(T_i)$	Sa at period of $T_i$ $T_1, T_2,$ and $T_3$ are the first, second, and third modes of vibration, respectively. $1.5T_1, 2T_1, 3T_1$ are the lengthened periods considering the effect of nonlinearity.
	$Sa_{avg}(T_i, T_j)$	The geometric mean of Sa between periods of $T_i$ and $T_j$
	$IM_c$	Mehanny and Cordova, $IM_c = Sa(T_1) \cdot \left( \frac{Sa(T_2)}{Sa(T_1)} \right)^{0.5}; T_2 = 2T_1$
	$I_{NP}$	Bojórquez and Iervolino, $I_{NP} = Sa(T_1) \cdot NP^{0.4}; NP = \frac{Sa_{avg}(T_1 \dots T_N)}{Sa(T_1)}; T_N = 2T_1$
	ASI	Acceleration spectrum intensity, $ASI = \int_{0.1}^{0.5} Sa(t) dT$
	VSI	Velocity spectrum intensity, $VSI = \int_{0.1}^{0.5} Sv(t) dT$
	HI	Housner Intensity, $HI = \int_{0.1}^{2.5} PSV(T) dT$
Peak-based IMs	PGA	
	PGV	Peak ground velocity
	PGD	Peak ground displacement
Cumulative and duration-based IMs	AI	Arias intensity, $AI = \frac{\pi}{2g} \int_0^{t_{max}} a(t)^2 dt$
	$D_{5-75}$	5-75% significant duration: The interval between the times at which 5% and 75% of Arias intensity are reached
	$I_D$	Cosenza and Manfredi index (a dimension less metric of duration) $I_D = \frac{\int_0^{t_{max}} a(t)^2 dt}{PGA \times PGV}$ Where $a(t)$ and $t_{max}$ are acceleration time history and the length of ground motion record, respectively
	CAV	Cumulative absolute energy, $CAV = \int_0^{t_{max}}  a(t)  dt$
	SED	Specific Energy Intensity ( $I_c$ )

with the mean value of  $\bar{S}$  for the short duration acceleration. The coefficient  $k = \frac{\bar{L}}{\bar{S}}$  was applied to short-duration acceleration. Among spectral equivalent candidates, acceleration with a lower total of squared differences (Equation (1)) was chosen as a spectral equivalent [6]:

$$SSE = \sum_{i=1}^{10} (L_i - kS_i)^2 \quad (1)$$

where  $L_i$  and  $S_i$  represent the acceleration of long and short ground motion duration, respectively.

In this research, a collection of acceleration, prepared by Chandrmohan et al. [6] was used. The

**TABLE 2.** Long- and short- duration ground motions characteristics (some parts of the table were adopted from [6])

Earthquake	Station name	$D_s$ 5-75 (s)	PGA (g)	Sa ( $T_1=0.74$ ) (g)	PGV (cm/s)	Specific Energy Density ( $\text{cm}^2/\text{sec}$ )	Housner Intensity (cm)	Acceleration Spectrum Intensity ( $\text{g} \cdot \text{sec}$ )	Velocity Spectrum Intensity (cm)	Epicentral distance Rjb (km)	
L1	1999 Kocaeli, Turkey	Bursa Tofas	26	0.101	0.276	17.236	1491.196	58.842	0.081	59.777	60.430
S1	1999 Chi- Chi, Taiwan- 04	KAU085	20	0.087	0.254	17.949	1227.339	57.281	0.075	58.852	85.950
L2	2010 Maule, Chile	Constitucion	32	0.538	1.084	43.347	9077.681	222.043	0.750	254.645	37.230
S2	1981 Taiwan SMART1(5)	SMART1 O12	1	0.579	0.818	62.441	1547.465	162.453	0.592	198.262	58.000
L3	2011 Tohoku, Japan	Inawashiro	80	0.280	0.525	46.649	14367.241	211.890	0.235	218.919	173.000
S3	1992 Erzincan, Turkey	Erzincan	2	0.282	0.577	78.149	3672.229	235.514	0.208	215.809	0.000
L4	2011 Tohoku, Japan	Naruko	71	0.208	0.263	32.982	17173.483	157.455	0.156	153.801	163.000
S4	1999 Chi- Chi, Taiwan- 06	TCU118	24	0.240	0.279	48.926	8161.988	166.889	0.200	160.738	26.820
L5	2011 Tohoku, Japan	Shiroishi	77	0.364	0.511	30.557	5421.761	175.801	0.354	186.388	161.000
S5	1979 Imperial Valley-06	El Centro Array #4	3	0.450	0.600	36.828	2491.399	165.401	0.337	175.011	4.900
L6	2011 Tohoku, Japan	Kakuda	69	0.360	0.874	46.056	9020.616	214.282	0.284	228.848	147.000
S6	1995 Kobe, Japan	Takarazuka	2	0.445	0.864	43.659	2044.341	201.162	0.326	202.496	0.000
L7	2011 Tohoku, Japan	Yonezawa	78	0.206	0.429	24.497	4397.940	123.421	0.228	128.399	153.000
S7	1999 Chi- Chi, Taiwan- 05	CHY063	13	0.213	0.445	26.512	1848.469	125.239	0.199	134.586	71.940
L8	2010 Maule, Chile	Concepcion San Pedro	32	0.607	1.478	41.449	9038.662	219.742	0.460	246.305	43.340
S8	1994 Northridge- 01	Sun Valley - Roscoe Blvd	6	0.612	1.173	58.484	4086.042	227.189	0.417	236.493	5.590
L9	2011 Tohoku, Japan	Inawashiro	80	0.280	0.525	46.649	14367.241	211.890	0.235	218.919	173.000

S9	1994 Northridge-01	Jensen Filter Plant	4	0.275	0.720	74.777	5145.300	202.983	0.196	189.680	0.000
L10	1985 Valparaiso, Chile	Llolleo	28	0.712	0.985	40.307	5393.310	196.723	0.603	223.045	N. A
S10	1994 Northridge-01	Sun Valley - Roscoe Blvd	6	0.504	0.829	46.293	3967.398	192.404	0.568	221.410	5.590
L11	2011 Tohoku, Japan	Iwanuma	80	0.366	0.808	48.983	14259.192	246.579	0.437	256.265	137.500
S11	1999 Chi-Chi, Taiwan-03	TCU138	5	0.470	0.827	53.360	4854.271	242.445	0.437	253.626	9.780
L12	2011 Tohoku, Japan	Sakunami	75	0.423	0.484	26.038	3093.641	98.835	0.447	114.983	155.000
S12	1999 Chi-Chi, Taiwan-02	TCU067	5	0.502	0.533	39.897	514.903	84.486	0.470	109.310	0.620
L13	2008 Wenchuan, China	Deyangbaima	36	0.139	0.184	35.632	4833.612	62.772	0.118	61.748	49.700
S13	1999 Chi-Chi, Taiwan-04	CHY016	23	0.131	0.188	21.757	2815.592	65.523	0.140	66.198	66.640
L14	2008 Wenchuan, China	Dayiyinping	60	0.138	0.201	32.839	2435.809	64.483	0.145	65.947	51.850
S14	1999 Chi-Chi, Taiwan	TTN051	24	0.128	0.187	24.500	2903.311	64.401	0.140	65.229	30.770
L15	2010 Maule, Chile	Curico	37	0.475	0.464	27.694	4299.173	144.484	0.463	159.697	61.700
S15	1983 Coalinga-01	Parkfield - Stone Co	5	0.527	0.559	41.247	1515.489	141.656	0.435	169.733	32.810
L16	2008 Wenchuan, China	Dayiyinping	47	0.129	0.262	19.960	1412.653	54.957	0.153	59.763	51.850
S16	2010 El Mayor-Cucapah	Sam W. Stewart	10	0.204	0.217	22.907	2758.602	51.907	0.166	56.156	31.790
L17	2011 Tohoku, Japan	Kaminoyama	86	0.125	0.301	15.716	2031.403	85.045	0.121	91.690	185.000
S17	1989 Loma Prieta	Los Gatos - Lexington Dam	2	0.149	0.337	28.931	355.682	84.341	0.108	92.256	3.600

selected acceleration is mentioned in Table 2. As an example, the characteristics of the two categories of accelerations were compared and their spectral acceleration adaptation is shown in Figures 2 and 3.

Although the selected pair records contained different strong ground motion durations, they were similar in terms of spectral response. The dependency of accelerations to various time intervals, with a distinction between long and short ground motion durations, is shown in Figure 4.

These records, in addition to being scaled and categorized based on strong ground motion duration, had other characteristics. Consequently, to better realize the dispersion of these intensity measures, the relationship between PGA, PGV,  $M_w$ , and  $S_a$  ( $T_1 = 0.74$ ) based on strong ground motion duration ( $D_{5-75}$ ) is shown in Figure 5. In Figure 6, the relationship between three important duration parameters, i.e.  $D_{5-75}$ ,  $M_w$ , and  $S_a$  ( $T_1 = 0.74$ ) is shown in all records.

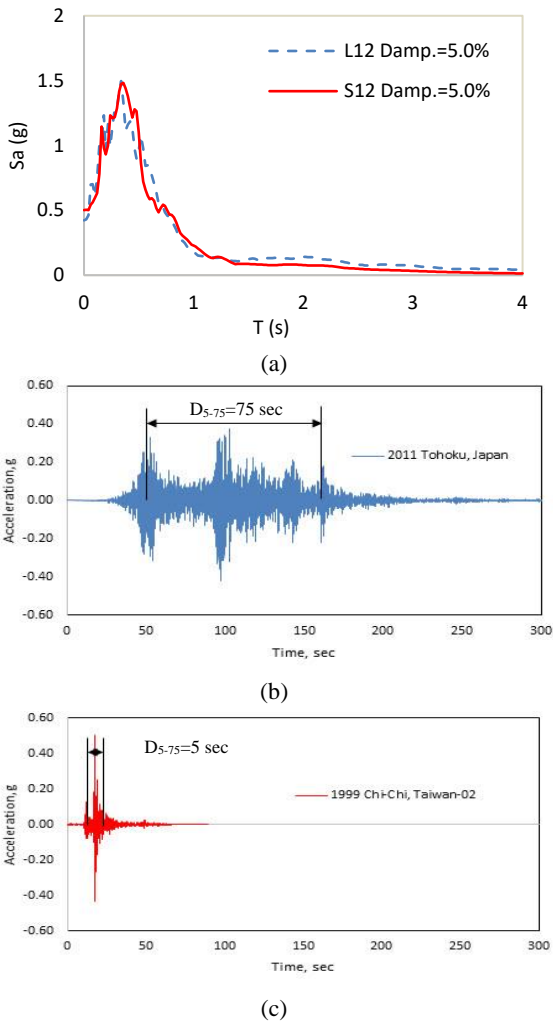


**Figure 2.** (a) Response spectra for earthquake record pair 12 b) Acceleration time-series for earthquake record pair 12 (Long duration) c) Acceleration time-series for earthquake record pair 12 (Short duration)

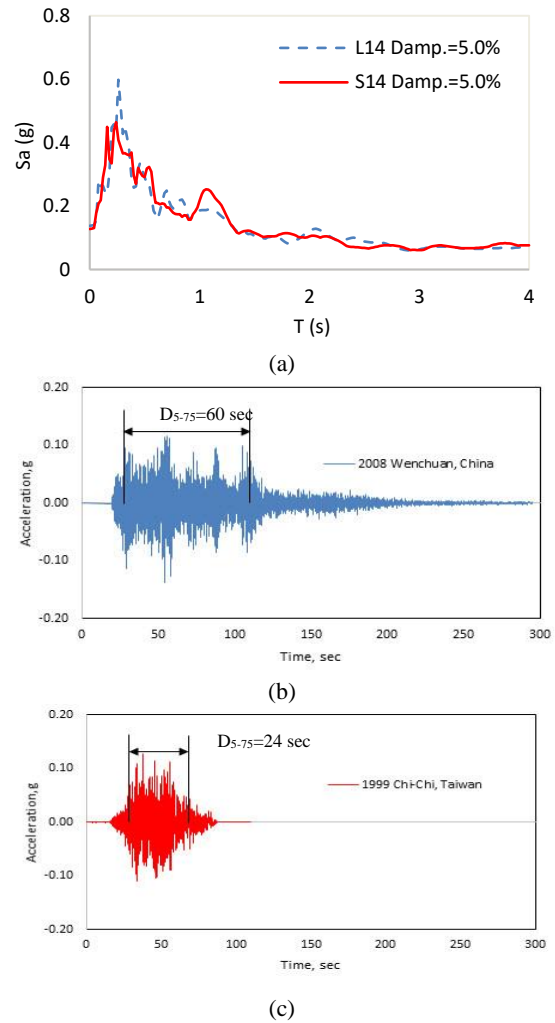


**Figure 3.** (a) Response spectra for earthquake record pair 14 b) Acceleration time-series for earthquake record pair 14 (Long duration) c) Acceleration time-series for earthquake record pair 14 (Short duration)

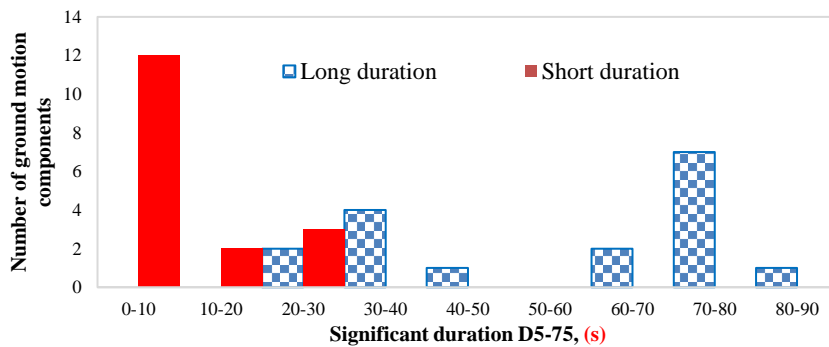


**Figure 4.** Histogram for all earthquake records used in this study (significant duration  $D_{5-75}$ )

An optimal dispersion between the acceleration spectrum and duration of the strong ground motion could

improve the results. In this regard, the correlation coefficient between the strong ground motion duration

and natural logarithm response spectrum at different periods was less than 0.2, as shown in Figure 7, indicating the optimal distribution between spectral accelerations at different periods and the strong ground motion duration. The purpose of correlation models is to examine the relationship between two or more variables, while regression seeks to predict one or more variables based on one or more other variables. Extensive use of the quantitative value of each of the seismic intensity measure criteria can be considered as its efficiency. The demand for each seismic intensity measure is obtained from Equation (2).

$$EDP=a (IM)^b \tag{2}$$

Equation (2) can be converted logarithmically with respect to the normal distribution. In this case, constant values can be obtained from the linear regression of the logarithmic equation. The efficiency of each intensity measure based on the residual dispersion ( $R^2$ ) is obtained from Equation (3).

$$\text{Log}^{(EDP)}=\text{Log}^{(a)} + b \text{Log}^{(IM)} \tag{3}$$

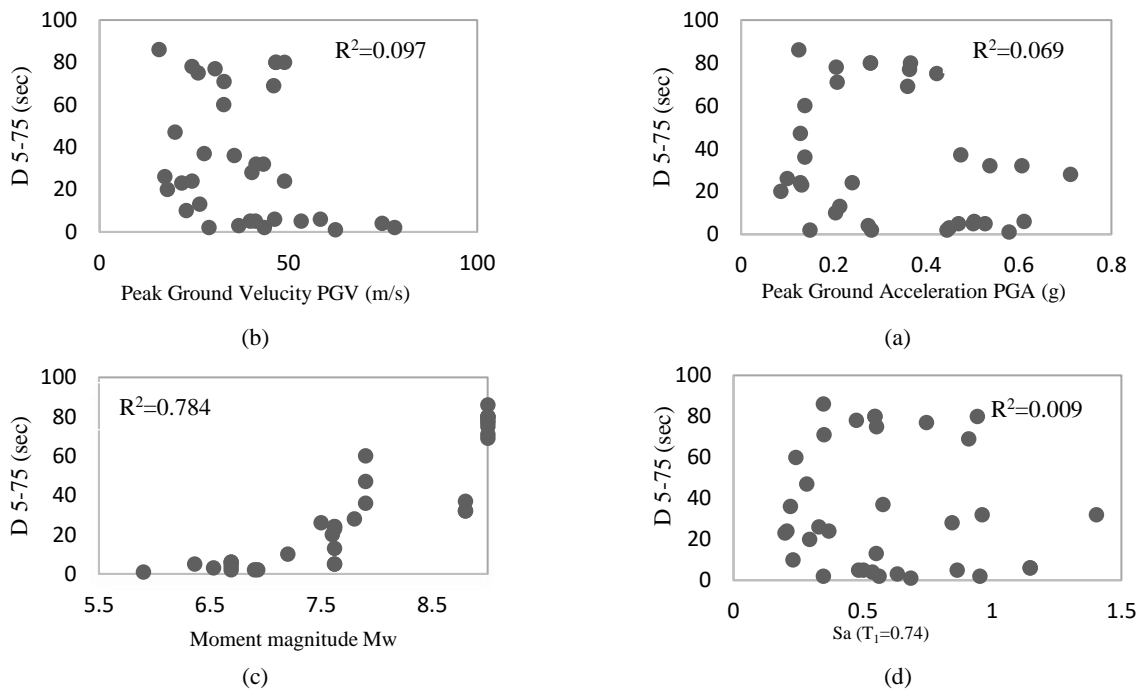


**Figure 5.** The relationship between intensity measures of: a) PGA to  $D_{5-75}$  b) PGV to  $D_{5-75}$  c)  $M_w$  to  $D_{5-75}$  d)  $D_{5-75}$

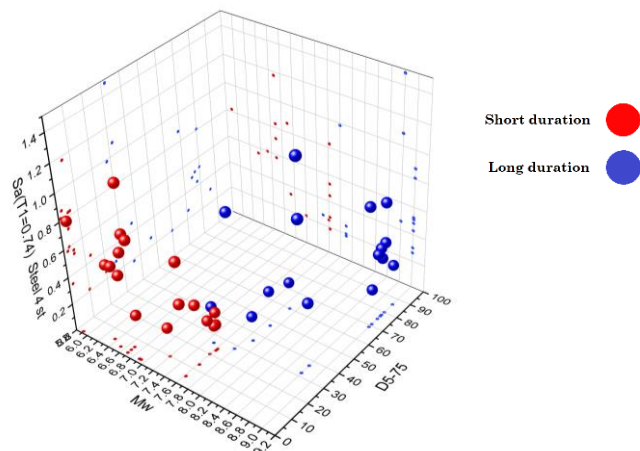


**Figure 6.** The relationship between intensity measures of  $M_w$ ,  $D_{5-75}$  and  $Sa(T_1=0.74)$



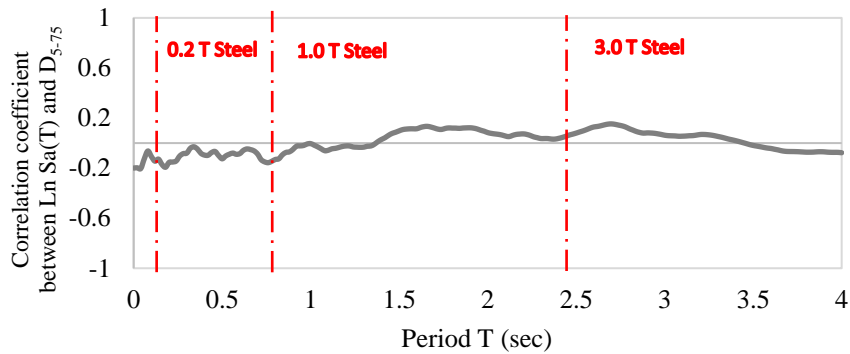


**Figure 7.** Correlation coefficient between significant duration,  $D_{5-75}$ , and natural logarithm of the spectral acceleration ( $S_a$ ) vs. period ( $T$ ) of vibration

**4. STUDIED MODEL**

**4. 1. General Descriptions** The steel structure used in this research consisted of four floors and was a regular, three-dimensional structure, made in the laboratory based on a real scale. It comprised two steel frames joined by beams with a 5-meter span. The height of the first floors was 3.2 meters and the other floors were 3.5 meters high. Figure 8 shows the laboratory sample of this structure. The design details and laboratory models are available in the reports Seismosoft [45]. Also, the details of the design, modeling, and constructing this laboratory model are achievable in reports [46]. In this study, verification of the result gained from maximum relative displacements at each level was carried out using laboratory observations of Pavan et al. [46], which is shown in Figure 8b.

The results of the modal analysis of the structures used in this study are summarized in Table 3.

**4. 2. Modeling and Analysis** Nonlinear analyses, especially dynamic analysis, are considered to be reliable and powerful tools in civil engineering practices [47–51]. In nonlinear modeling, beam and column elements were modeled using displacement-based fiber-section as shown in Figure 9. For steel materials, the initial stiffness and strength were assumed to decrease when hysteresis cycles continued. Steel sections were divided into approximately 100 fibers, following the Menegotto-pinto behavioral diagram. Also, columns and beams have been modeled through 3D displacement-based inelastic frame elements [46]. The modeled sections would automatically consider the two-way axial and flexural force coexistence. Shear and torsion in a cross-section were assumed to be uncoupled linear elastic. As a result, in the analysis of beam and column elements, the decay in stiffness and strength was ignored while the behavior was derived from shear and torsion. Floors were considered to be rigid diaphragms. Gravity loads and seismic masses at the joints of beams and columns were

applied based on the dependent tributary area of each node. The damping ratio of 5% for the first and higher-mode, and Rayleigh-type damping according to mass and tangent stiffness properties was taken into account. Hilber-Hughes-Taylor Integration scheme was used to analyze time history.



**Figure 8.** (a) Four storey 3D steel moment resisting frame [46]

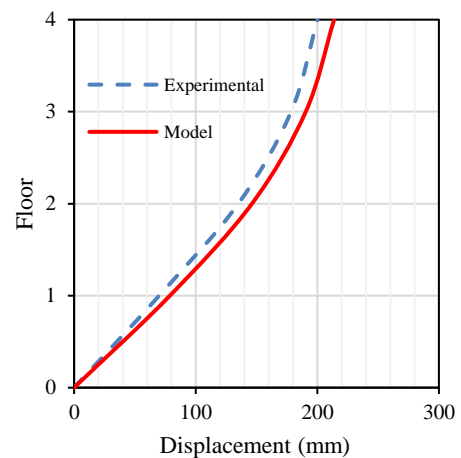
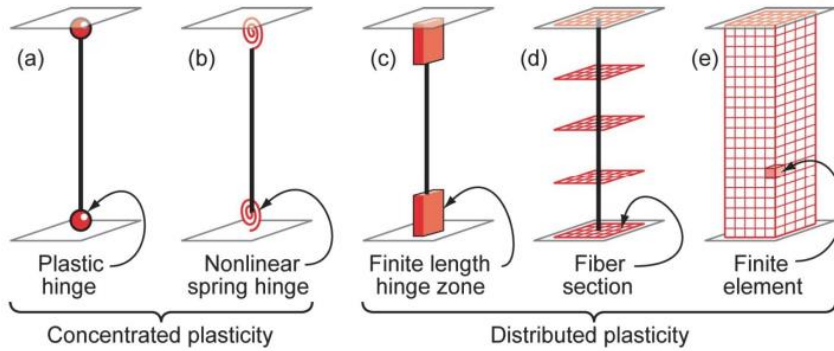
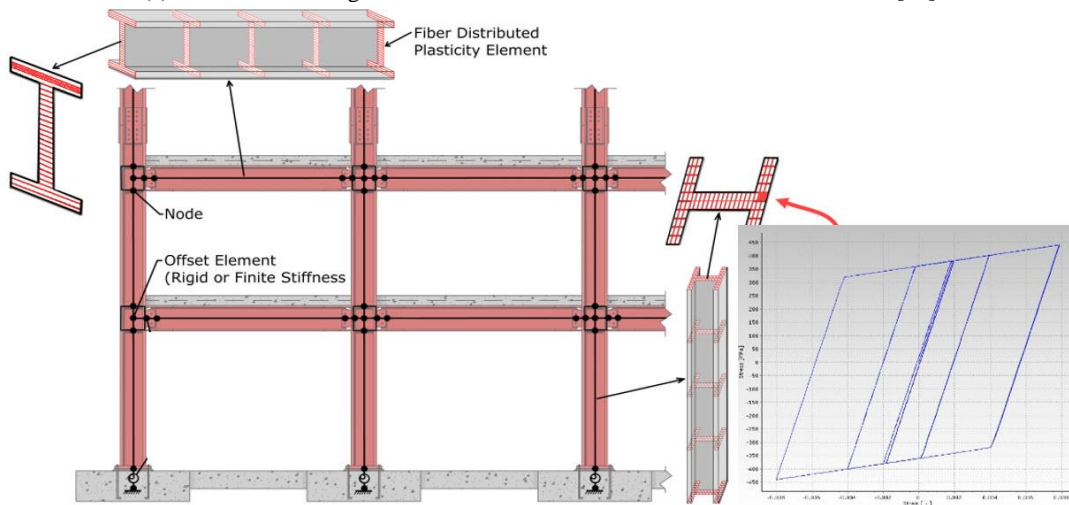


**Figure 8.** (b) Validation results of the experimental model and the model made in the software



(a) Idealized modeling of nonlinear behavior of deformation control members [47]



(b) Typical force-displacement diagram for bilinear steel model and hierarchical levels of distributed plasticity FE models [54]

**Figure 9. Structural Modeling**

**TABLE 3.** Numerical model and experiment specimen modal properties of the four-storey steel building

Mode	Periods of vibration (T)	Effective modal mass		
		UX (%)	UY (%)	RZ (%)
1	0.741	84.6	0.0	0.0
2	0.731	0.0	85.1	0.0
3	0.668	0.0	0.0	85.2
4	0.1379	0.0	3.3	0.0
5	0.1375	3.2	0.0	0.0

The nonlinear time history analysis as the most accurate numerical structural analysis [47,52] was performed using SeismoStruct 2016 software [53]. Since there were two record categories, each containing 17 records, to optimize the process of analyzing and evaluating the performance of the structure in nonlinear ranges, the 34 records were scaled so that the structure would reach its collapse threshold in each record. This considerably increased both the number of analysis operations and the accuracy of the results.

## 5. RESULTS AND DISCUSSION

### 5.1. The Correlation between Seismic Parameters of Earthquakes

After extracting the seismic parameters of the records whose corresponding values are shown in Table 3, the correlation between each seismic parameters was investigated. Then, the correlation was represented quantitatively for seismic parameters of the observed records, using the correlation concept previously discussed. The matrices derived from the

relationships between various seismic parameters in two categories of accelerations with long (Li) and short (Si) duration of motion are summarized in Tables 4 and 5. As shown in Tables 4 and 5, the highest PGA (Peak ground acceleration) correlation was related to AI (Arias intensity) and ASI (Acceleration spectrum intensity), which was the same in both long duration and short duration categories of records. The correlation coefficient in both short and long term categories showed a weak correlation between PGA and PGV/PGA ratio, and SED (Specific Energy Density). PGV (Peak ground velocity) showed a strong correlation with most of the seismic parameters, the weakest correlation with PGV/PGA ratio, and the strongest correlation in both cases with HI (Housner Intensity). In general, PGV has a desirable correlation with energy-dependent seismic parameters. The results of the correlation of PGD (Peak ground displacement) seismic parameter showed that the dispersion was relatively high in the correlation of this parameter and the other seismic parameters. The least dispersion in both short and long term durations was related to energy-dependent parameters.

In examining seismic parameter PGV/PGA, although there was a weak correlation between this parameter and

other seismic parameters, the dispersion of correlation in both short and long durations was very low, and the results were close to each other. A relatively strong correlation between AI and most of the seismic parameters was observed. The best parameters indicating the status of this parameter were PGA and ASI, which were similar in the results of both short and long term analyses. The results obtained from the seismic parameter analysis of SED showed a weak correlation between this parameter and other seismic parameters. The correlations were lower in short-term analysis than in the long-term one. Meanwhile, this parameter showed a relatively good correlation with PGV and HI. Due to the definition of the duration of Arias affecting ASI, the strong correlation of this parameter with PGA and AI could be predicted. This parameter would show a good correlation with energy-related parameters VSI and HI. The correlation of VSI with all of the seismic parameters, except PGV/PGA, was high, but data dispersion in both short and long term durations was not high. The strongest correlation between the studied parameters was related to VSI and HI, being very similar to each other. The results of analyzing this seismic parameter were slightly more in the long-duration than the short one.

**TABLE 4.** Correlation between seismic parameters of earthquake for Long ground-motion duration

	PGA	PGV	PGD	PGV/PGA	Arias Intensity	SED	ASI	VSI	HI
PGA	1								
PGV	0.50	1							
PGD	0.35	0.18	1						
PGV/PGA	-0.78	-0.01	-0.20	1					
Arias Intensity	0.90	0.56	0.23	-0.71	1				
SED	0.20	0.75	0.07	0.04	0.31	1			
ASI	0.91	0.45	0.15	-0.76	0.96	0.15	1		
VSI	0.74	0.82	0.25	-0.52	0.79	0.69	0.70	1	
HI	0.68	0.83	0.22	-0.45	0.73	0.75	0.63	0.99	1

**TABLE 5.** Correlation between seismic parameters of earthquake for Short ground-motion duration

	PGA	PGV	PGD	PGV/PGA	Arias Intensity	SED	ASI	VSI	HI
PGA	1								
PGV	0.52	1							
PGD	-0.25	0.25	1						
PGV/PGA	-0.66	0.27	0.42	1					
Arias Intensity	0.75	0.38	-0.14	-0.51	1				
SED	0.00	0.45	0.64	0.33	0.24	1			
ASI	0.94	0.43	-0.28	-0.68	0.85	-0.03	1		
VSI	0.75	0.80	0.12	-0.17	0.67	0.41	0.66	1	
HI	0.61	0.84	0.25	0.00	0.53	0.51	0.50	0.98	1

**5. 2. Comparison of the Residual Inter-story Drift (RIDR)**

Since the records were matched for both short- and long-duration ones in terms of the response spectra, the acceleration applied to the structure was expected to be similar in both short and long durations. Therefore, by comparing the effect of the two accelerations with the same response spectra but different durations, we could ascertain the effect of duration on the response of the structures. Figure 10 shows how the residual inter-story drift ratio (RIDR) could change in the twenty pairs of records (L14, S14).

As shown in Figure 10 (b), RIDR was larger in the long time mode (L14) than the short mode (S14). As shown in Figure 10 (a),  $S_a(T_1)$  was greater in L14 than S14 at the period of 0.74 seconds, which was related to the structure under analysis. This could be due to larger  $S_a(T_1)$  at the period of 0.74 second (the period of structure analysis), long duration of strong ground

motion, and the reduction in the stiffness and strength of structural members in acceleration cycles.

**5. 3. Comparison of Different Intensity Measures**

As mentioned previously, an efficient IM can predict the seismic response of structures with low dispersion. In this research, different intensity measures were compared according to RIDR, in long and short duration of strong motion. Figures 11-21 show the severity of the intensity measures based on RIDR in different duration modes in addition to the correlation coefficient ( $\rho$ ) and regression ( $R^2$ ) of these intensity measures.

Although the  $S_a(T_1)$  intensity measure (IM) is the most useful parameter, the use of this intensity measure is less reliable in the range of nonlinear behavior where the stiffness of the structure decreases and the period of the structure increases compared to the linear behavior.

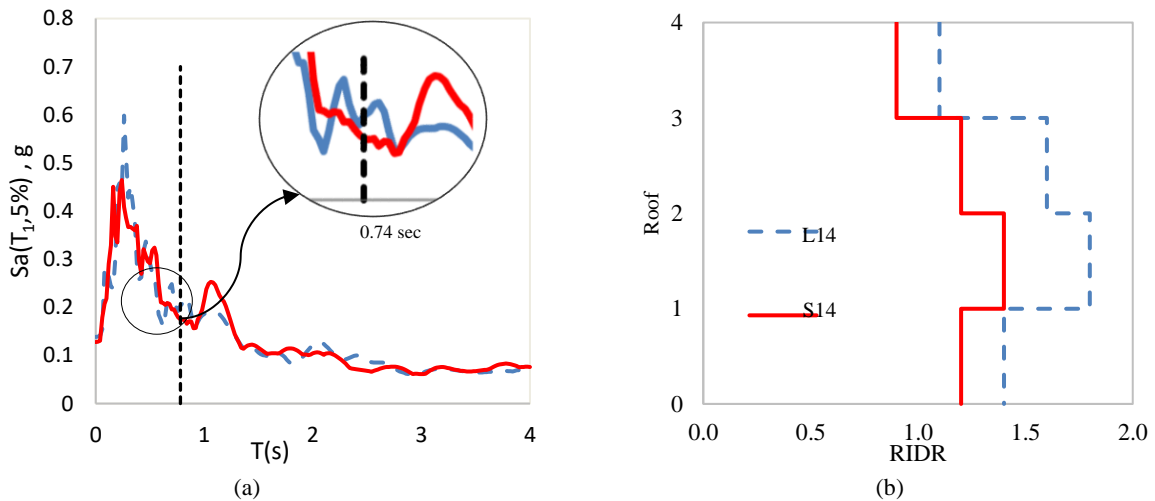


Figure 10. a)  $S_a(T_1, 5\%)$  curve for L14 and S14 records b) the comparison of RIDR for L14 and S14 records

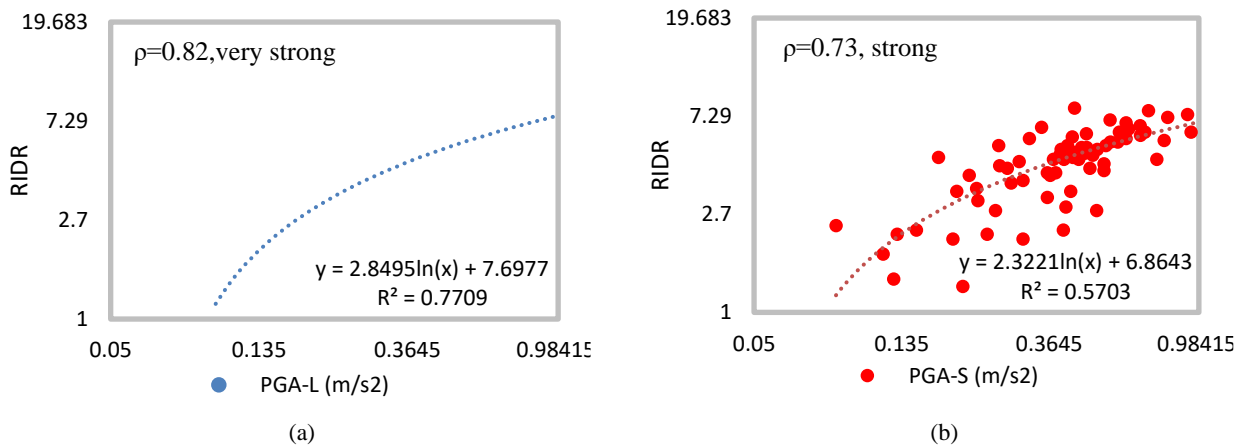
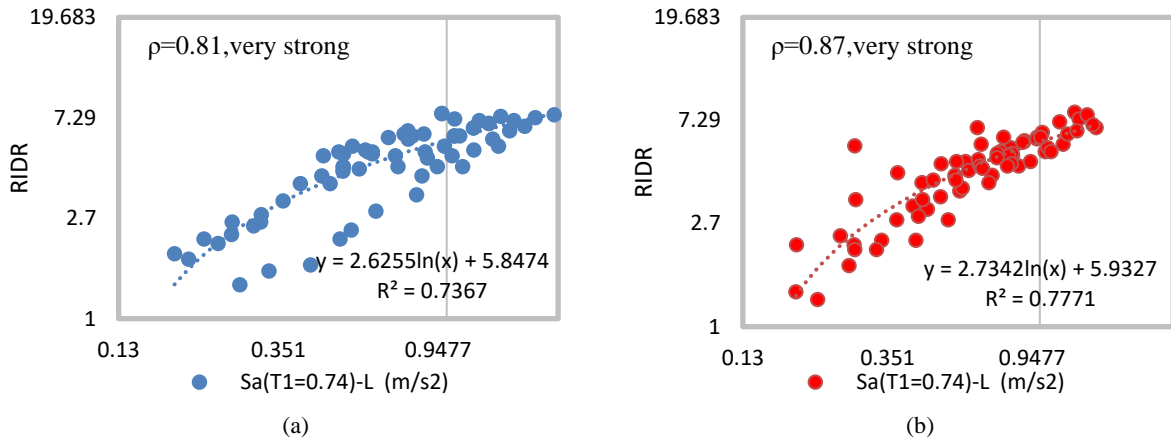
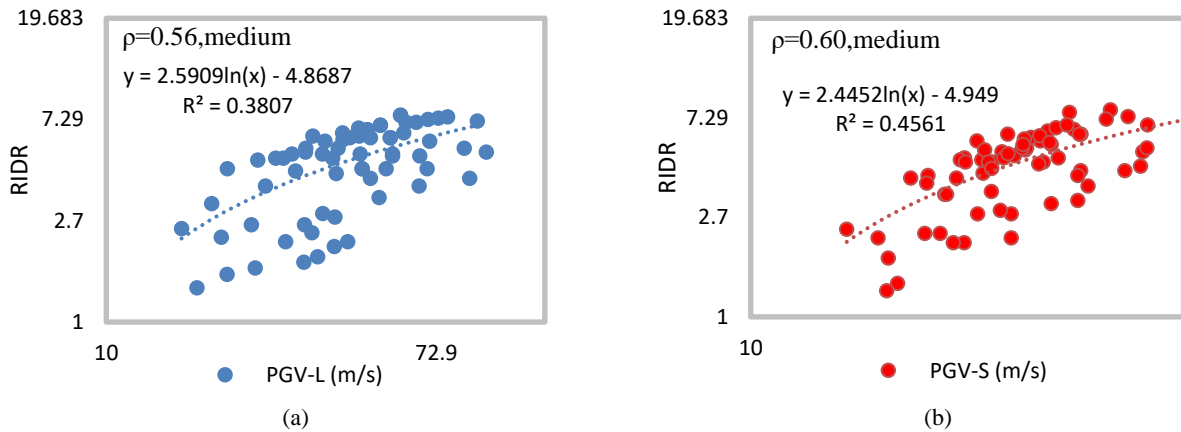


Figure 11. RIDR to Intensity measure of PGA curve for: a) Long ground-motion duration and b) Short ground-motion duration



**Figure 12.** RIDR to Intensity measure of  $Sa(T_1=0.74)$  curve for: a) Long ground-motion duration and b) Short ground-motion duration



**Figure 13.** RIDR to Intensity measure of PGV curve for: a) Long ground-motion duration b) Short ground-motion duration

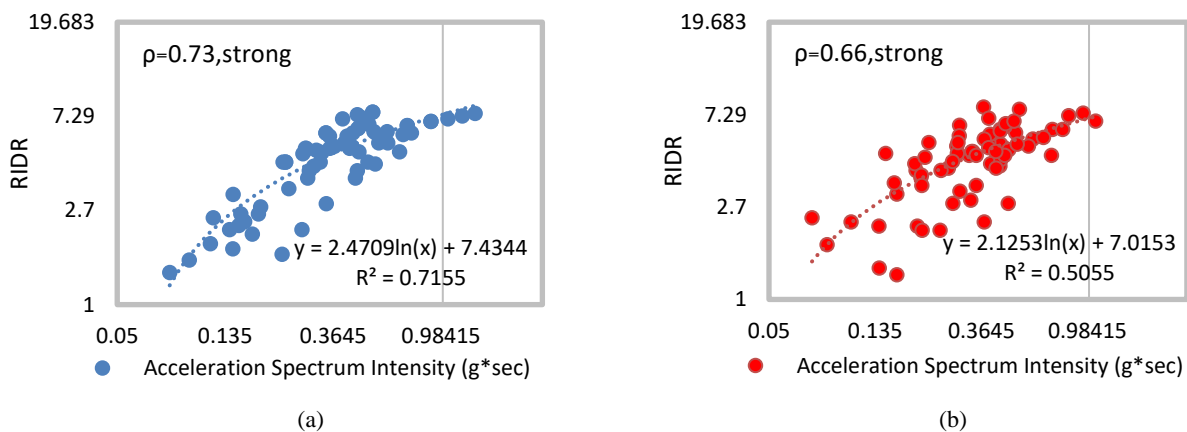


**Figure 14.** RIDR to Intensity measure of ASI (Acceleration Spectrum Intensity) curve for: a) Long ground-motion duration b) Short ground-motion duration

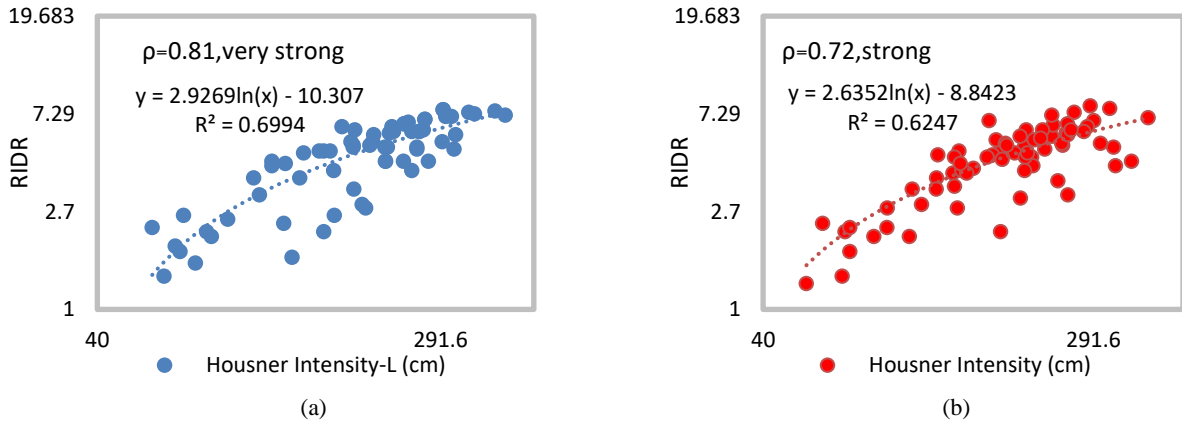


**Figure 15.** RIDR to Intensity measure of HI (Housner Intensity) curve for: a) Long ground-motion duration b) Short ground-motion duration

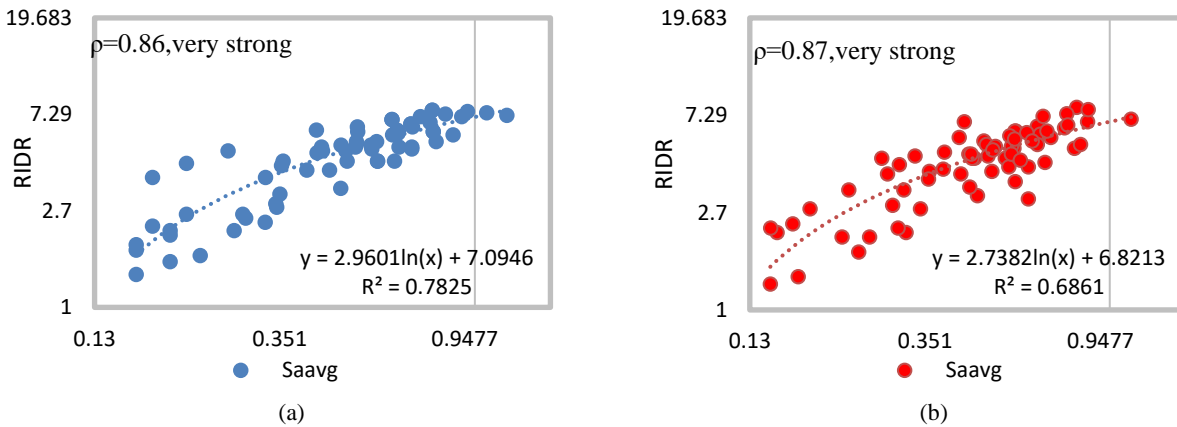


**Figure 16.** RIDR to Intensity measure of  $S_{avg}$  curve for: a) Long ground-motion duration b) Short ground-motion duration

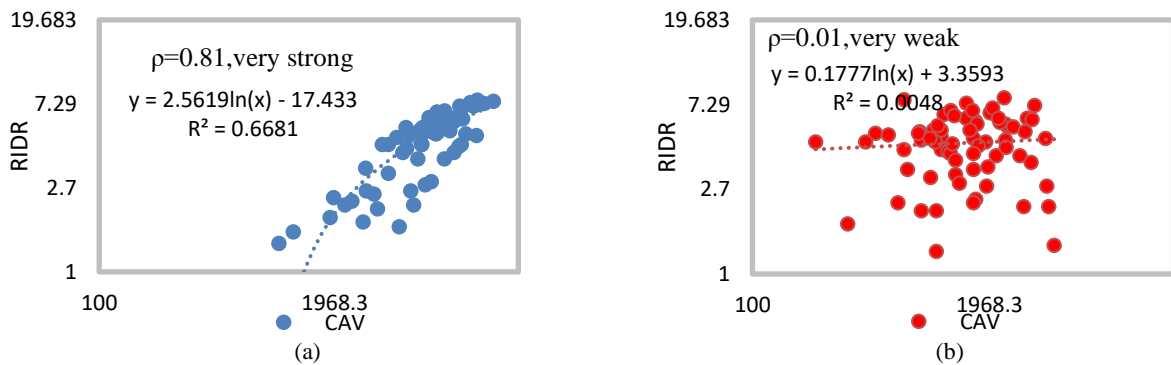


**Figure 17.** RIDR to Intensity measure of CAV (Cumulative absolute energy) curve for: a) Long ground-motion duration b) Short ground-motion duration

Increasing the period due to nonlinear behavior causes the structure to be affected by a range of response spectra different from values corresponding to the first mode period of the structure. Therefore, the appropriate

intensity measure is a parameter that in addition to the spectral acceleration component at the time of the first mode of the structure, considers a component of the spectral acceleration at the time of period greater than the

time of the first mode of the structure. Accordingly, the use of INP intensity measure is recommended to evaluate the seismic performance of structures in nonlinear problems. In this intensity measure, a part of the response spectrum that has a great effect on the nonlinear behavior of the structure is considered as a part of the intensity measure. Therefore, this IM was considered to evaluate the residual drift of the stories due to the ground motion duration. Finally, a comparison was made between the efficiency of intensity measure in predicting nonlinear behavior and residual drift.

Figures 11-21 show the RIDR variations in different values of intensity measures in long and short durations

of ground motion in detail. In each figure, the regression ( $R^2$ ) shows the amount of RIDR dispersion for each variation in different intensity measures. The correlation coefficient ( $\rho$ ) also specifies the degree of correlation of the data in each intensity measure. For example, in Figure 11, which illustrates the extent of RIDR variations in different PGA values, it is clear that as PGA increased, RIDR rose, too; however, the increase was more in the long term duration record mode than the short term one. The strong correlation coefficient in both forms would enhance the reliability of the results.

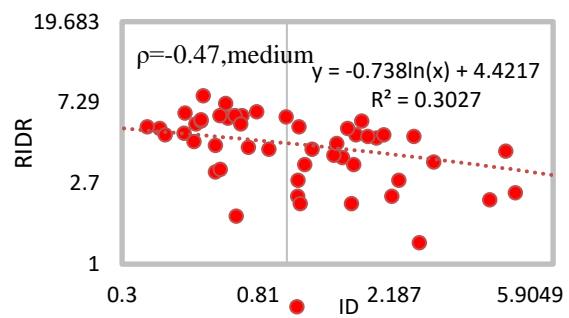
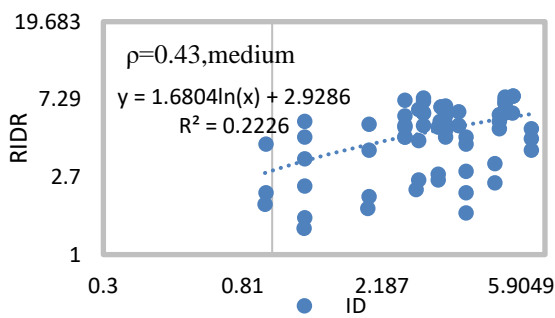


Figure 18. RIDR to Intensity measure of  $I_D$  curve for: a) Long ground-motion duration b) Short ground-motion duration

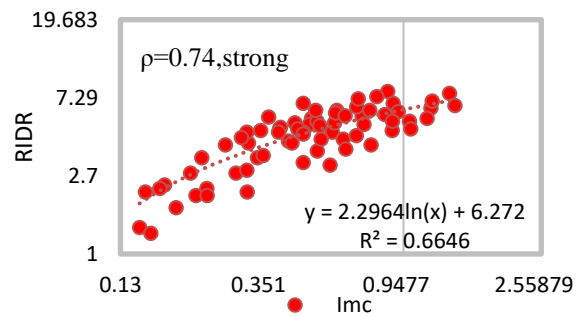
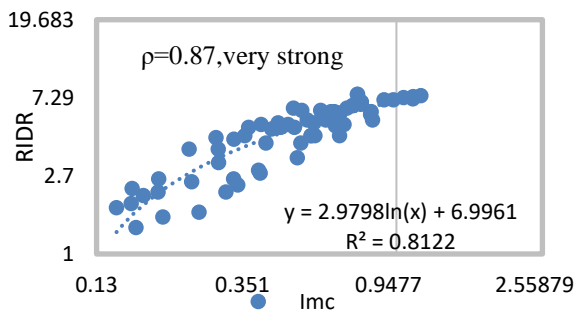


Figure 19. RIDR to Intensity measure of  $I_{mc}$  curve for: a) Long ground-motion duration b) Short ground-motion duration

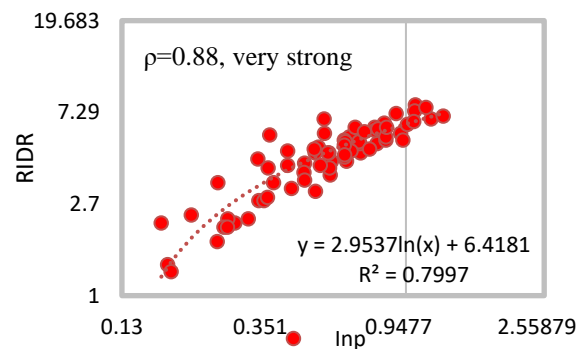
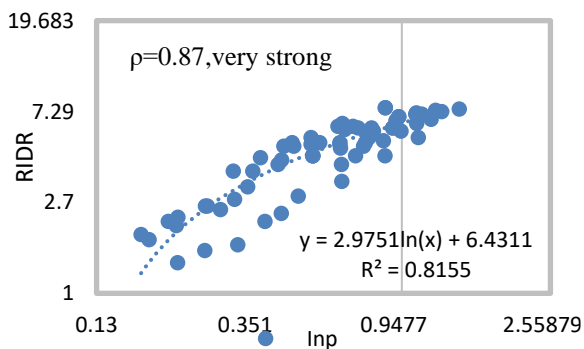


Figure 20. RIDR to Intensity measure of  $I_{NP}$  curve for: a) Long ground-motion duration b) Short ground-motion duration



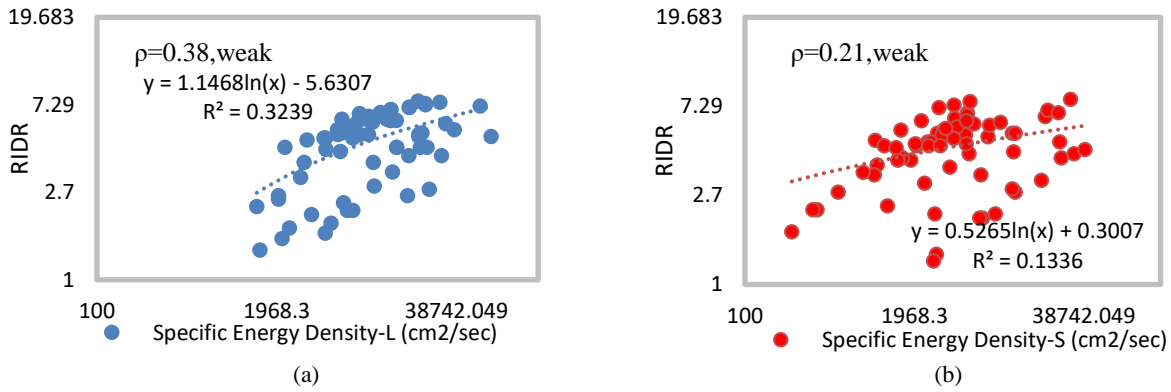


Figure 21. RIDR to Intensity measure of SED curve for: a) Long ground-motion duration b) Short ground-motion duration

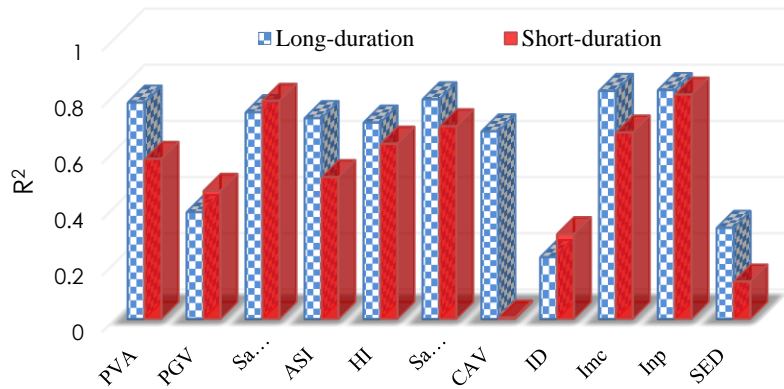


Figure 22. The comparison of regressions of intensity measures for the Long- and short-duration ground motion

In general, among eleven intensity measures in ten cases with an increase in various intensity measures, the RIDR ascended in both long- and short-durations strong ground motion. Only in  $I_D$ , and in the short term, a declining trend was observed. This could be due to the direct relationship between this intensity measure and the Arias duration which is one of the bases in sorting the records. In Figure 22, the comparison of intensity measures for the Long- and short- ground motion duration is shown. How various intensity measures affected RIDR in the long-duration motion mode could be as follows:

$$I_{NP} > IM_c > S_{a_{ave}} > PGA > S_a(T_1) > ASI > HI > CAV > PGV > SED > I_D$$

And in the short-duration motion mode as:

$$I_{NP} > S_a(T_1) > S_{a_{ave}} > IM_c > HI > PGA > ASI > PGV > I_D > SED > CAV$$

## 6. CONCLUSION

In this study, the impact of strong ground motion duration on the seismic response of a three dimensional model was investigated with respect to different types of intensity

measures. Two sets of long- and short-duration natural earthquake records were utilized to discover the impact of strong ground motion duration on the seismic response of the abovementioned structure. In addition, the effect of different intensity measures on the response of the structure was assessed and the adequacy of the intensity measures was calculated. Utilizing correlation coefficients, the dependency of seismic parameters was surveyed. Indeed, in this research, the correlation between seismic parameters of earthquakes, quantitative comparison of RIDR and the effect of different intensity measures on the 4-floor steel structure of the RIDR were investigated under two acceleration categories with long and short ground motion duration. The following results can be highlighted:

1. The results showed that domain-based seismic parameters, such as PGA, PGV and, PGD could have a direct relationship with energy-based seismic parameters, e.g. AI, SED, ASI, VSI, and HI. This direct relationship is associated with relatively strong correlations, being higher in PGA relationships with more energy-based seismic parameters than PGV and PGD. The quantitative results indicated that PGV / PGA showed a direct relationship with other seismic



parameters, but a weak correlation was observed, which was more important in long-duration. Generally, PGA, HI, and VSI, in addition to a direct relationship with other seismic parameters (except PGV / PGA), represented the strongest correlation with other seismic parameters of both short- and long-duration ground motions.

2. Comparing RIDR in long and short strong ground motion duration modes indicated that with an increase in the duration, the RIDR would rise.
3. 11 intensity measures were compared in terms of long and short strong ground motion duration with regard to RIDR. The quantitative results, mentioned in section 5-3, showed that most of the intensity measures were directly related to RIDR (except  $I_D$ ). In other words, with an increase in intensity measure, RIDR would rise. In general, in long-duration strong ground motions,  $I_{NP}$ ,  $IM_c$ , and  $S_{a_{ave}}$  intensity measures showed the least dispersion (highest regression) with RIDR, indicating that RIDR tended to increase with a steep rise in this magnitude. However, for the short-duration strong ground motions,  $I_{NP}$ ,  $S_a(T_1)$  and  $S_{a_{ave}}$  intensity measures caused the least dispersion. The results of the mentioned intensity measures indicated the strongest correlation among intensity measures of the surveyed, which could predict the response of structures at low dispersion.

## 7. REFERENCES

1. Hancock J, Bommer JJ, Eeri M. "Earthquake Engineering Practice A State-of-Knowledge Review of the Influence of Strong-Motion Duration on Structural Damage", *Earthquake Spectra*, 2006;22:827-845. doi:10.1193/1.2220576.
2. Raghunandan M, Liel AB, Luco N. "Collapse risk of buildings in the Pacific northwest region due to subduction earthquakes" *Earthq Spectra*, (2015), Vol. 31, 2087-2115.
3. Chester D.K. "The 1755 Lisbon earthquake." *Progress in Physical Geography*, Vol. 25, No. 3 (2001), 363-383. doi:10.1177/030913330102500304.
4. Bradley BA. Strong ground motion characteristics observed in the 4 September 2010 Darfield, New Zealand earthquake. *Soil Dynamics and Earthquake Engineering*, Vol. 42, (2012), 32-46. doi:10.1016/j.soildyn.2012.06.004.
5. Hamidi H, Jamnani, Amiri JV, Rajabnejad H. Energy distribution in RC shear wall-frame structures subject to repeated earthquakes, *Soil Dynamics and Earthquake Engineering*, Vol. 107, (2018), 116-128. doi:10.1016/j.soildyn.2018.01.010.
6. Chandramohan R, Baker JW, Deierlein GG. Quantifying the influence of ground motion duration on structural collapse capacity using spectrally equivalent records, *Earthquake Spectra*, Vol. 32, No. 2, (2016). doi:10.1193/1.22813EQS298MR2.
7. Barbosa AR, Ribeiro FLA, Neves LAC. Influence of earthquake ground-motion duration on damage estimation: application to steel moment resisting frames", *Earthquake Engineering & Structural Dynamics*, Vol. 46, No. 1 (2017), 27-49. doi:10.1002/eqe.2769.
8. Ruiz-García J. "On the influence of strong-ground motion duration on residual displacement demands", *Earthquake and Structures*, Vol. 1, No. 4, (2010), 327-344. doi:10.12989/eas.2010.1.4.327.
9. Song R, Li Y, van de Lindt J.W. "Impact of earthquake ground motion characteristics on collapse risk of post-mainshock buildings considering aftershocks", *Engineering Structures*, Vol. 81, (2014), 349-361. https://doi.org/10.1016/j.engstruct.2014.09.047.
10. Foschaar JC, Baker JW, Deierlein GG. "Preliminary assessment of ground motion duration effects on structural collapse" Proc. 15th World Conference. Earthquake Engineering, 2012.
11. Raghunandan M, Liel AB. "Effect of ground motion duration on earthquake-induced structural collapse" *Structural Safety*, Vol. 41, (2013), 119-133. https://doi.org/10.1016/j.strusafe.2012.12.002.
12. Hancock J, Bommer JJ. "Using spectral matched records to explore the influence of strong-motion duration on inelastic structural response. Soil", *Dynamics and Earthquake Engineering*, Vol. 27, (2007), 291-299. doi:https://doi.org/10.1016/j.soildyn.2006.09.004.
13. Zhang S, Wang G, Pang B, Du C. "The effects of strong motion duration on the dynamic response and accumulated damage of concrete gravity dams. Soil", *Dynamics and Earthquake Engineering*, Vol. 45, (2013), 112-124. doi:10.1016/j.soildyn.2012.11.011.
14. Bommer JJ, Magenes G, Hancock J, Penazzo P. "The influence of strong-motion duration on the seismic response of masonry structures" *Bulletin of Earthquake Engineering*, Vol. 2, No. 1, (2004), 1-26. https://doi.org/10.1023/B:BEEE.0000038948.95616.bf.
15. Iervolino I, Manfredi G, Cosenza E. Ground motion duration effects on nonlinear seismic response. *Earthquake Engineering & Structural Dynamics*, Vol. 35, No. 1, (2006), 21-38. doi:10.1002/eqe.529.
16. Bojorquez E, Iervolino I, Manfredi G, Cosenza E. Influence of ground motion duration on degrading SDOF systems. In First European Conference on Earthquake Engineering and Seismology (2006), 3-8.
17. Nassar AA, Krawinkler H. Seismic demands for SDOF and MDOF systems, John A. Blume Earthquake Engineering Center, Republished 1991;95. (Doctoral dissertation, Stanford University, 1991).
18. Shome N, Cornell CA, Bazzurro P, "Carballo JE. Earthquakes, records, and nonlinear responses", *Earthquake Spectra* 1998;14:469-500. doi:https://doi.org/10.1193/1.1586011.
19. Tremblay R, Atkinson GM. "Comparative Study of the Inelastic Seismic Demand of Eastern and Western Canadian Sites" *Earthquake Spectra*, (2001), Vol. 17, 333-358. doi:10.1193/1.1586178.
20. Chai YH. "Incorporating low-cycle fatigue model into duration-dependent inelastic design spectra", *Earthquake Engineering & Structural Dynamics*, Vol. 34, No. 1, (2005), 83-96. doi:10.1002/eqe.422.
21. Bhargavi P, Raghukanth STG. "Rating damage potential of ground motion records", *Earthquake Engineering & Engineering Vibration*, Vol. 18, No. 2, (2019), 233-254. doi:10.1007/s11803-019-0501-1.
22. Bradley BA. Correlation of significant duration with amplitude and cumulative intensity measures and its use in ground motion selection. *Journal of Earthquake Engineering*, Vol. 15, No. 6, (2011), 809-832. doi:10.1080/13632469.2011.557140.
23. Zhou J, Tang K, Wang H, Fang X. Influence of ground motion duration on damping reduction factor. *Journal of Earthquake*

- Engineering*, Vol. 18, No. 5, (2014), 816-830. doi:10.1080/13632469.2014.908152.
24. Bejejo A, Barbosa AR, Bento R. "Influence of ground motion duration on damage index-based fragility assessment of a plan-symmetric non-ductile reinforced concrete building", *Engineering Structures*, Vol. 151, (2017), 682-703. <https://doi.org/10.1016/j.engstruct.2017.08.042>.
  25. Baker JW, Cornell CA. "Vector-valued ground motion intensity measures for probabilistic seismic demand analysis", Pacific Earthquake Engineering Research Center, College of Engineering, Stanford University; 2006.
  26. Mazza F, Labernarda R. "Structural and non-structural intensity measures for the assessment of base-isolated structures subjected to pulse-like near-fault earthquakes. Soil", *Dynamics and Earthquake Engineering*, Vol. 96, (2017), 115-127. doi:10.1016/j.soildyn.2017.02.013.
  27. Zhou Y, Ge P, Han J, Lu Z. "Vector-valued intensity measures for incremental dynamic analysis. Soil", *Dynamics and Earthquake Engineering*, Vol. 100, (2017), 380-388. doi:10.1016/j.soildyn.2017.06.014.
  28. Yakhchalian M, Nicknam A, Amiri GG. "Optimal vector-valued intensity measure for seismic collapse assessment of structures", *Earthquake Engineering & Engineering Vibration*, Vol. 14, No. 1, (2015), 37-54. doi:10.1007/s11803-015-0005-6.
  29. Kassem MM, Nazri FM, Farsangi EN. "The efficiency of an improved seismic vulnerability index under strong ground motions", *Structures*, Vol. 23, Elsevier; (2020), 366-382. doi:<https://doi.org/10.1016/j.istruc.2019.10.016>.
  30. Kassem MM, Nazri FM, Farsangi EN. "On the quantification of collapse margin of a retrofitted university building in Beirut using a probabilistic approach", *Engineering Science and Technology, an International Journal*, Vol. 23, No. 2, (2020), 373-381. doi:<https://doi.org/10.1016/j.jestch.2019.05.003>.
  31. Farsangi EN, Yang TY, Tasnimi AA. "Influence of concurrent horizontal and vertical ground excitations on the collapse margins of non-ductile RC frame buildings", *Structural Engineering and Mechanics*, Vol. 59, No. 4, (2016), 653-669. doi:<http://dx.doi.org/10.12989/sem.2016.59.4.653>.
  32. Nazri FM, Miari MA, Kassem MM, Tan C-G, Farsangi EN. "Probabilistic evaluation of structural pounding between adjacent buildings subjected to repeated seismic excitations", *Arabian Journal for Science and Engineering*, Vol. 44, No. 5 (2019): 4931-4945. doi:<https://doi.org/10.1007/s13369-018-3666-4>.
  33. Yakhchalian M, Ghodrati Amiri G. "A vector intensity measure to reliably predict maximum drift in low-to mid-rise buildings", *Proceedings of the Institution of Civil Engineers-Structures and Buildings*, Vol. 172, No. 1 (2019), 42-54. doi:<https://doi.org/10.1680/jstbu.17.00040>.
  34. Luco N, Cornell CA. "Structure-specific scalar intensity measures for near-source and ordinary earthquake ground motions", *Earthquake Spectra*, (2007), Vol. 23, 357-392. doi:10.1193/1.2723158.
  35. Lee BJ, Chou TY, Hsiao CP, Chung LK, Huang PH, Wu YB. "The statistics and analysis of building damage on Chi-Chi earthquake" International Train Programs Seismic Design Building Structure Taipei, Taiwan National Center Research Earthquake Engineering, 2002.
  36. Mehanny SS, Cordova PP. "Development of a two-parameter seismic intensity measure and probabilistic design procedure" *Journal of Engineering Applied Science*, Vol. 51, (2004), 233-252.
  37. Bojórquez E, Iervolino I. "Spectral shape proxies and nonlinear structural response. Soil", *Dynamics and Earthquake Engineering*, Vol. 31, (2011), 996-1008. doi:10.1016/j.soildyn.2011.03.006.
  38. Soleymani Abed. Investigation of Correlations between Seismic Parameters and Damage Indices for Earthquakes of Iran Region (TECHNICAL NOTE). *International Journal of Engineering, Transactions B: Applications*, Vol. 27, (2014), 283-292, doi:10.5829/idosi.ije.2014.27.02b.12
  39. Bommer JJ, Martinez-Pereira A. "The effective duration of earthquake strongmotion", *Journal of Earthquake Engineering*, (1999), Vol. 3, 127-172. doi:<https://www.worldscientific.com/doi/abs/10.1142/S1363246999000077>.
  40. Pagratis D. Prediction of earthquake strong ground-motion for engineering use. M Sc Diss 1995.
  41. Sarma SK. "Energy flux of strong earthquakes", *Tectonophysics* Vol. 11, No. 3 (1971), 159-173. doi:[https://doi.org/10.1016/0040-1951\(71\)90028-X](https://doi.org/10.1016/0040-1951(71)90028-X).
  42. Ghodrati AG, Mahmoudi H, Razavian ASA. "Probabilistic seismic hazard assessment of Tehran based on Arias intensity", *International Journal of Engineering, Transactions B: Applications* Vol. 23, No. 1, February 2010: Pp 1-20. doi:<https://www.sid.ir/en/journal/ViewPaper.aspx?id=177545>.
  43. Boore DM. On pads and filters: Processing strong-motion data. *Bulletin of the Seismological Society of America*, Vol. 95, No. 2 (2005), 745-750. doi:<https://doi.org/10.1785/0120040160>.
  44. Boore DM, Bommer JJ. "Processing of strong-motion accelerograms: needs, options and consequences", *Soil Dyn Earthquake Engineering*, (2005), Vol. 25, 93-115. doi:<https://doi.org/10.1016/j.soildyn.2004.10.007>.
  45. SeismoSoft, SeismoStruct. "A computer program for static and dynamic nonlinear analysis of framed structures." *Disponível online em: http://www.seissoft.com* (2006).
  46. Pavan A, Pinho R, Antoniou S. "Blind prediction of a full scale 3D steel frame tested under dynamic conditions" 14th World Conf. Earthquake Engineering, Beijing, China, Oct., 2008.
  47. Deierlein GG, Reinhorn AM, Willford MR. Nonlinear structural analysis for seismic design. NEHRP Seismic Design Technical Brief, No. 4, 2010;1-36.
  48. Ghodrati Amiri G, Hamidi Jamnani H, Ahmadi HR. "The Effect of Analysis Methods on the Response of Steel Dual-System Frame Buildings for Seismic Retrofitting", *International Journal of Engineering, Transactions B: Applications*, Vol. 22, No. 4 (2009), 317-331. <https://www.sid.ir/en/journal/ViewPaper.aspx?ID=165187>.
  49. Nicknam A, Mosleh A, Hamidi Jamnani H. "Seismic performance evaluation of urban bridge using static nonlinear procedure, case study: Hafez bridge" *Procedia Engineering*, Vol. 14, 2011. doi:10.1016/j.proeng.2011.07.296.
  50. Jalilkhani M, Manafpour AR. "A simplified modal pushover analysis-based method for incremental dynamic analysis of regular rc moment-resisting frames", *International Journal of Engineering, Transactions B: Applications*, Vol. 31, No. 2, (2018), 196-203. doi:10.5829/idosi.ije.2015.28.02b.04.
  51. Baharmast H, Razmyan S, Yazdani A. "Approximate incremental dynamic analysis using reduction of ground motion records", *International Journal of Engineering, Transactions B: Applications*, Vol. 28, No. 2, (2015), 190-197. doi:10.5829/idosi.ije.2015.28.02b.04.
  52. Hamidi H, Khosravi H, Soleimani R. "Fling-step ground motions simulation using theoretical-based Green's function technique for structural analysis. Soil", *Dynamics and Earthquake Engineering*, Vol. 115, (2018), 232-245. <https://doi.org/10.1016/j.soildyn.2018.08.023>.
  53. Sadeghi A, Abdollahzadeh G, Rajabnejad H, Naseri SA. "Numerical analysis method for evaluating response modification factor for steel structures equipped with friction dampers", *Asian Journal of Civil Engineering*, Vol. 22, No. 2, (2021), 313-330. doi:<https://doi.org/10.1007/s42107-020->

00315-2.

54. NIST (National Institute of Standards and Technology).

"Guidelines for Nonlinear Structural Analysis for Design of Buildings Part Iia-Steel Moment Frames." (2017). (NIST GCR 17-917-46v2).

---



---

### Persian Abstract

---

**چکیده**

در ارزیابی عملکرد سازه‌ها در هنگام زلزله، ویژگی‌های مدت زمان موثر حرکت قوی زمین بر روی پاسخ سازه‌ها تا حدی مبهم باقی مانده و دارای نتایج غیر قطعی می‌باشند. سنجه شدت (IM) رابطه‌ای بین خطر حرکت زمین با پاسخ سازه ایجاد می‌کند. از این رو، استفاده از IM مناسب نقش مهمی در پیش‌بینی پاسخ سازه دارد. در این تحقیق، تأثیر مدت زمان حرکت قوی زمین و ضریب همبستگی سنجه شدت‌های مختلف، بر روی جابجایی نسبی باقیمانده بین طبقات (RIDR) یک سازه فولادی سه بعدی مورد بررسی قرار گرفته است. با استفاده از تحلیل دینامیکی غیرخطی و ۳۴ رکورد زلزله، رابطه بین پارامترهای لرزه‌ای مدت زمان حرکت قوی زمین در دو حالت کوتاه و بلند شامل دامنه، انرژی و پارامترهای محتوای فرکانسی مورد ارزیابی قرار گرفت. همچنین، همبستگی بین ۱۴ سنجه شدت اسکالر و جابجایی نسبی باقیمانده بین طبقات RIDR سازه نیز بررسی شده است. نتایج نشان داده است که بیشترین همبستگی بین پارامترهای لرزه‌ای همچون HI، VSI و PGA با دیگر پارامترها در هر دو حرکت قوی زمین با مدت زمان کوتاه و بلند وجود دارد. براساس شاخص حداکثر دررفت باقیمانده بین طبقات، سنجه شدت‌های INP، IMC و Saave کمترین پراکندگی در برابر رکوردهای مدت زمان بلند را دارا بوده‌اند. از سوی دیگر، معیارهای شدت Sa(Ti) و Saave کمترین پراکندگی را در برابر رکوردهای مدت زمان کوتاه نشان داده است.

---